Journal Pre-proof

Elucidation of metal and support effects during ethanol steam reforming over Ni and Rh based catalysts supported on (CeO_2)-ZrO_2-La_2O_3

Marinela D. Zhurka (Investigation) (Writing - original draft), Angeliki A. Lemonidou (Resources) (Writing - review and editing), Panagiotis N. Kechagiopoulos (Conceptualization) (Methodology) (Writing - review and editing) (Supervision)

PII: S0920-5861(20)30139-5

DOI: https://doi.org/10.1016/j.cattod.2020.03.020

Reference: CATTOD 12733

To appear in: *Catalysis Today*

Received Date: 30 November 2019

Revised Date: 24 February 2020

Accepted Date: 13 March 2020

Please cite this article as: Zhurka MD, Lemonidou AA, Kechagiopoulos PN, Elucidation of metal and support effects during ethanol steam reforming over Ni and Rh based catalysts supported on (CeO_2)-ZrO_2-La_2O_3, *Catalysis Today* (2020), doi: https://doi.org/10.1016/j.cattod.2020.03.020

Elucidation of metal and support effects during ethanol steam reforming over Ni and Rh based catalysts supported on (CeO_2)-ZrO_2-La_2O_3

Marinela D. Zhurka,[1] Angeliki A. Lemonidou,[2] Panagiotis N. Kechagiopoulos[1]*

[1]Chemical and Materials Engineering Group, School of Engineering, University of Aberdeen, Aberdeen, AB24 3UE, UK

[2]Laboratory of Petrochemical Technology, Department of Chemical Engineering, Aristotle University of Thessaloniki, GR-54124 Thessaloniki, Greece

* Corresponding author: p.kechagiopoulos@abdn.ac.uk

Graphical abstract

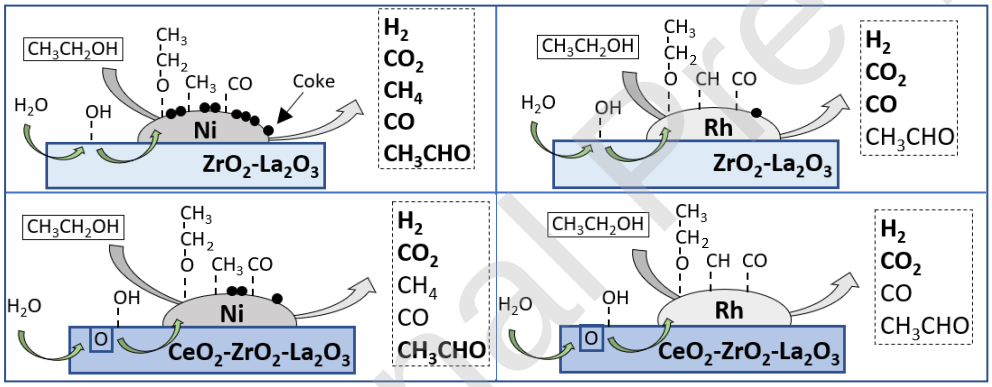

Highlights

- ESR studied on Ni and Rh catalysts supported on (CeO_2)-ZrO_2-La_2O_3 mixed oxides.
- Dehydrogenation reactions favoured on Rh catalysts, leading to zero CH_4 production.
- Steam dissociation on ZrO_2 enhances activity and selectivity versus inert supports.
- High oxygen mobility in CeO_2 containing supports promotes water gas shift reaction.
- Rh/CeO_2-ZrO_2-La_2O_3 exhibits the highest performance and lowest carbon deposition.

Abstract

Hydrogen production via steam reforming of biomass derived oxygenates is a promising environmental alternative to the use of fossil fuels. The ethanol steam reforming reaction is investigated over Ni and Rh based catalysts supported on ZrO_2-La_2O_3 and CeO_2-ZrO_2-La_2O_3 mixed oxides, aiming at the elucidation of the role of the metal and the support in the reaction mechanism. Rh versus Ni is shown to be highly active and more selective with no methane production under all conditions studied. CeO_2-ZrO_2-La_2O_3 versus ZrO_2-La_2O_3 is shown to promote efficiently the water gas shift reaction, enhancing hydrogen production substantially. Time on stream studies show that the catalysts on ceria containing supports are highly stable, whereas a gradual deactivation was more evident on the ZrO_2-La_2O_3 supported catalysts. TPO analysis of spent catalysts revealed extremely low amounts of graphitic coke deposited on the Rh catalysts. On Ni, and particularly the ZrO_2-La_2O_3 supported catalyst, larger peaks corresponding to both amorphous and graphitic coke were evident, amounting to higher coke production. The combined effects of metal and support make the catalysts on CeO_2-ZrO_2-La_2O_3 most suitable for the reaction, with Rh/CeO_2-ZrO_2-La_2O_3 showing particularly high activity, selectivity and stability, with minimal CH_4 and CO production resulting at the highest H_2 yield.

Keywords: Ethanol steam reforming; Nickel; Rhodium; Ceria-Zirconia-Lanthana; Mixed oxides; Support effect

1. Introduction

The increasing energy demand along with the finite supply of fossil fuels and pollution problems, stemming from the extensive use of the latter, have intensified research on alternative renewable energy sources [1]. Hydrogen is a clean energy carrier with high energy density that can be used for the production of electricity in fuel cells or heat. Most of the hydrogen originates currently from fossil fuels, resulting in high CO_2 emissions with well-known negative impacts on the environment [2]. Biomass conversion to hydrogen has the potential to accelerate the latter's realization as a major, carbon neutral, energy carrier [3]. Out of various liquid sources for hydrogen, bio-ethanol is a sustainable candidate with low toxicity and easy handling [4].

Ethanol steam reforming is an endothermic reaction producing CO_2 and H_2, with its reaction pathway shown to strongly depend on the catalyst [5–9] and operating conditions [10,11]. Several parallel reactions take

place on the surface of the catalyst along with reforming, resulting in the generation of different by-products, such as acetaldehyde, ethylene, methane, carbon monoxide, acetone and carbon deposits [12]. Dehydrogenation, dehydration, decomposition and polymerization reactions, as presented in various kinetic studies [13], contribute to the formation of these by-products. Due to the complexity of the reaction pathway H_2 production is affected by the operating conditions, with maximum ethanol conversion and H_2 yield being achieved at high temperatures, S/C ratios and contact times [14].

Both transition [15–17] and noble [18–20] metals have been extensively examined as catalysts for ESR reactions, indicating that ethanol activation pathways depend on the metal nature. Rh based catalysts are considered as the most active due to their excellent C-C and C-H bond scission affinity, high water gas shift (WGS) activity and high resistance towards carbon deposition [21,22]. The reaction pathway over Rh based catalysts is primarily steered by the metal's oxophilicity leading to the dehydrogenation of ethanol to acetaldehyde, followed by decomposition reactions to yield CH_x and CO species [23]. The CH_x fragments further dehydrogenate on the metal active sites to C species which are most likely to be oxidized to CO_x, thus low CH_4 and high CO_x selectivities are observed [24]. However, the high cost of noble metals has shifted the attention to transition metals such as Ni, with various studies suggesting the latter metal as active for ESR given its effectiveness in catalysing C-C and C-O bond scissions. Ethanol adsorbed on Ni active sites can dehydrogenate towards acetaldehyde, followed by decomposition reactions for the formation of CH_3 and CO species [25–27]. These methyl groups at lower temperatures desorb as CH_4, with nickel's methanation activity also contributing to higher methane selectivities. Over all metals, acid sites on the support can promote in parallel ethanol's dehydration towards ethylene [28], while carbon deposition remains a major issue for the long term stability of Ni catalysts [29,30].

The study of supports based on CeO_2-(ZrO_2) has received particular interest on account of ceria's redox properties that facilitate the formation of surface and bulk oxygen vacancies, the latter effectively replenished by water from the feed [31]. The well-known oxygen storage capacity of CeO_2 and the associated supply of O species to the metal can enhance the oxidation of carbonaceous fragments on the surface of the catalyst and promote the WGS and reforming reactions [32]. Conversion and the H_2 yield are enhanced, while

by-products such as CH_4 and coke precursors are largely eliminated [33]. Zirconia supports are of interest independently, due to the oxide's ability to dissociate water molecules and provide hydroxyl species to the metal [34]. Lastly, among used modifiers, La_2O_3 is known to enhance the stability of Ni catalysts through strong metal–support interactions (SMSI), that lead to an enhancement of the dissociation of water [35] and the mobility of O species in CeO_2 supports [31]. The enhanced catalytic stability during ESR over Ni catalysts with the addition of La_2O_3 has also been reported, attributed to the formation of thin overlayers of La_2O_x on top of Ni particles [36]. Upon reaction with CO_2 the formed lanthanum oxycarbonate reacts with surface carbon cleaning the Ni surface from carbonaceous deposits.

Recently [37], Ni and Rh catalysts supported on ZrO_2-La_2O_3 or CeO_2-ZrO_2-La_2O_3 showed high activity at short contact times in methane and biogas steam reforming at the 400-550^{o}C range, with the CeO_2-ZrO_2-La_2O_3 supported ones further exhibiting notably stable behaviour at extended 90 h stability tests. The present study reports on the steam reforming of ethanol over these catalysts at a wide range of experimental conditions in a fixed bed reactor, focusing on the investigation of the effect of both the metal and the support on the catalytic activity and selectivity, but also stability and coke formation. The CeO_2-ZrO_2-La_2O_3 supported catalysts are revealed to be particularly stable and active for the reaction, achieving very high H_2 yields at 400^{o}C. Turnover frequencies over the Ni sample outperform most literature reported values on Ni catalysts, approaching those of the much more expensive noble metal Rh, highlighting the promise of this catalyst for industrial application.

2. Experimental procedures

2.1. *Catalysts preparation and characterisation*

The preparation procedures of catalyst samples and their characterisation has been reported in detail in previous studies relating to methane steam reforming [37]. Nickel and Rhodium catalysts supported on ceria and lanthana doped zirconium oxide (0% or 17% CeO_2 and 5% La_2O_3) provided by Mel Chemicals were prepared via the wet impregnation method using $Ni(NO_3)_2{\cdot}6H_2O$ and $RhCl_3{\cdot}3H_2O$ as precursors for Ni (10 wt%) and Rh (1 wt%). N_2 adsorption at 77 K, using the multipoint BET analysis method with an Autosorb-1 Quantachrome flow apparatus was used to measure the surface area of prepared catalysts. X-ray diffraction

(XRD) patterns were obtained using a Siemens D500 diffractometer, with Cu Kα radiation, in order to identify the crystalline phases apparent. Temperature programmed reduction (TPR) and desorption (TPD) were performed in a gas flow system using a U-tube reactor connected online with a quadrupole mass analyzer (Omnistar) to study the reducibility and the metal dispersion of the catalysts. Coke deposits on spent catalyst samples were characterised by means of Temperature Programmed Oxidation (TPO) analysis conducted on a Thermo Scientific TPDRO 1100 instrument with a TCD detector. In all TPO experiments, spent catalyst samples were pre-treated in a He flow at 250^{o}C for 30 min and then allowed to cool to 40^{o}C. The temperature was subsequently increased to 800^{o}C at a rate of 5^{o}C min^{-1} under a flow of 20 cm^{3} min^{-1} of 10% O_2 in He.

2.2. ***Reactor setup***

The study took place in a fully automated reaction system by PID Eng & Tech (Micro Activity-Effi unit). An HPLC pump (Gilson 307) delivered the ethanol/water feed, the latter channelled through an evaporator in the hot box of the unit, operating at 150^{o}C, and further mixed with N_2, fed via a mass flow controller (Bronkhorst El-Flow Select). Reaction products were fed into a Gas/Liquid separator, operated at 0^{o}C, to separate and collect condensables. Analysis of the gas products took place on-line in a HP 5890 GC equipped with a TCD detector and MS–5A and HS–T columns, using N_2 as the internal standard, while liquids were analysed off-line in a Thermo Scientific TRACE 1300 GC using an FID detector and a TG WAXMS A column.

A quartz fixed bed reactor (10 mm i.d. and total length 370 mm) was used for all experiments, heated by a single-zone furnace, able to provide an isothermal region of 5 cm. A fitted porous plate ensured that the catalyst bed remained in the furnace's isothermal zone. A thermocouple inside the reactor in a fixed position of 5 mm above the porous plate was used for temperature measurement and control. The catalyst was diluted with α-Al_2O_3 granules while quartz wool was placed at both ends to support the bed in the tube.

2.3. ***Experimental conditions and parameters***

Prior each experiment the catalyst was reduced using a flow of 5% H_2 on N_2 for 1 h at 550^{o}C (determined via TPR to be a sufficient reduction temperature for all catalysts). Reaction temperature was varied over a range of 300-600^{o}C at an inlet molar Steam/Carbon (S/C) ratio of 3 and a GHSV of 2.78 s^{-1} (calculated at NTP conditions as total gas equivalent flow). The effect of partial pressure of ethanol was studied varying the

latter from 0.06 to 0.37 bara at 400°C and a GHSV of 1.78 s^{-1}, keeping the partial pressure of water constant at 0.74 bara. Similarly, the effect of partial pressure of water was studied over a range of 0.26 to 1.56 bara at 400°C and a GHSV of 2.36 s^{-1}, at a constant partial pressure of ethanol of 0.13 bara. In both cases, these ranges were equivalent to a S/C variation of 1 to 6, while a N_2 flow was used to maintain constant the volumetric flow rate. The space time effect was studied at 400°C at a S/C ratio of 3, varying the ratio of the catalyst mass over the mass flow rate of ethanol, $W/F_{Eth,t0}$, from 58 to 349 g_{cat} s g_{Eth}^{-1}, by changing the ethanol and water feed over a fixed mass of catalyst and flow of N_2 resulting in variation of the GHSV from 3.89 to 0.64 s^{-1}. Stability runs were carried out in the same reaction system at a temperature of 500°C and S/C of 3, at a space time of 358 g_{cat} s g_{Eth}^{-1} (GHSV = 1.08 s^{-1}). A mass of 80 mg of catalyst was used in all experiments.

A minimum of three replicate experiments were carried out for most conditions to verify the repeatability of results, while at the start and end of every experimental session the performance of the catalyst was evaluated at reference conditions (temperature of 400°C and S/C of 3) to ensure significant deactivation had not occurred. Atomic C, H and O mass balance closure in all tests was in the order of 100 ± 5%. The results presented in following sections are the average values from the replicate experiments and are expressed in terms of the parameters shown below, whereas in Table S2 of the Supporting Information the respective standard deviations are also provided in tabular form.

Conversion: $X_{Eth} = \frac{F_{Eth}^{in} - F_{Eth}^{out}}{F_{Eth}^{in}} \times 100$

Carbon selectivity of compound y with n carbon atoms: $S_c(y) = \frac{0.5nF_y^{out}}{F_{Eth}^{in} - F_{Eth}^{out}} \times 100$

Hydrogen yield: $Y_{H_2} = \frac{F_{H_2}^{out}}{6F_{Eth}^{in}} \times 100$

Turnover Frequency: $TOF = \frac{F_{Eth}^{in} - F_{Eth}^{out}}{N_{Surf,Ni}}$

with $N_{Surf,Ni}$ being the moles of surface Ni as obtained from H_2-TPD and F_i^x being the molecular flowrate of compound i.

Results are also compared with thermodynamic equilibrium at equivalent conditions, calculated via Gibb's free energy minimisation using the Aspen Plus software with the Peng-Robinson equation of state; considering ethanol, water, carbon monoxide, carbon dioxide, methane, hydrogen and acetaldehyde as compounds.

3. Results and Discussion

3.1. *Catalyst characterisation*

The characterization of the catalysts used in this work has been reported in previous studies [37,42], hence in the present section only a summary of main results is presented. Table S1 in the Supporting Information presents the specific surface area and metal dispersion of the catalysts, while diffraction patterns are shown in Figure S1. Crystalline phases identified in the supports were $Zr_{0.84}Ce_{0.16}O_2$ for CeO_2-ZrO_2-La_2O_3 and ZrO_2 for ZrO_2-La_2O_3. In both cases, no La_2O_3 peaks were observed most probably due to the latter's amorphous state or fine dispersion. The characteristic peaks of the respective supports and those of NiO are present in the XRD patterns of the Ni-based catalysts. In the case of the Rh-based catalysts, no peaks for Rh_2O_3 were detected, most likely due to its low content. The TPR profiles of the catalysts and the supports are shown in Figure S2. Relatively mild conditions are sufficient for the reduction of all catalysts, with approximately 180°C and 480°C needed for the Rh-based and the Ni-based catalysts, respectively. A low intensity peak at 340°C was also observed in the TPR profile of the CeO_2-ZrO_2-La_2O_3 support, ascribed to the partial reduction of ceria, whereas no reduction peak was visible in the case of the ZrO_2-La_2O_3 support.

3.2. *Effect of temperature*

The effect of temperature on ESR over all catalysts tested is presented in Figure 1, where ethanol conversion and H_2 yield are both seen to increase with the rise of temperature. Different conversions are achieved depending on the support and metal used, evidencing an effect of both on the obtained performances. In all cases, results are far from thermodynamic equilibrium, which predicts the conversion of ethanol even at 300°C to be complete. CeO_2-ZrO_2-La_2O_3 supported catalysts are the most active, with the Rh one being clearly the most performant. Comparing the current results with equivalent obtained over Ni supported on inert

SiO_2 from our previous work [25], the beneficial effect of the supports used is clear, particularly at the lower temperatures. Indicatively, at 300°C ethanol conversion was as low as 5% on Ni/SiO_2, whereas it reached values of 18 and 23% over the ZrO_2-La_2O_3 and the CeO_2-ZrO_2-La_2O_3 supported Ni catalysts, respectively. This comparison becomes even more favourable for the current catalysts when the respective surface areas (37.17 and 45.07 m^2/g for the ZrO_2-La_2O_3 and CeO_2-ZrO_2-La_2O_3 versus 105.32 m^2/g for the SiO_2 one) are taken into account. The promoting effect of CeO_2 on the performance of the Ni catalysts is further underlined upon consideration of the lower surface area and dispersion of the CeO_2-ZrO_2-La_2O_3 supported catalyst in comparison to the ZrO_2-La_2O_3 supported one. Over Rh, performance enhancement was even larger, with the CeO_2 containing catalyst achieving a comparatively much higher conversion of 36% at the same temperature of 300°C. Moreover, this catalyst remained visibly more active in relation to all others across the entire temperature range studied, whereas differences for the rest were not as large at higher temperatures.

Further evidence on the effect of the support and metal on performances obtained are provided by the products carbon selectivities presented in Figure 2. For all catalysts, acetaldehyde is identified as a major intermediate, derived from the dehydrogenation of ethanol, aligning well with both experimental observations [31,43] and theoretical predictions [44]. CeO_2 has been reported to also be able to dissociate ethanol towards ethoxy species, the latter dehydrogenating to acetaldehyde or reacting with available O species on the support's surface towards acetate [31,45]. However, the overall similar selectivities of acetaldehyde observed over SiO_2 supported Ni [25] suggest that its formation is primarily driven by metal catalysed ethanol dehydrogenation.

Notable, are also the very low CH_4 selectivities achieved (Figure 2c) for all catalysts across the entire temperature range investigated. On Ni based catalysts the selectivity of methane never exceeded 6%, with the lowest values being consistently obtained over the CeO_2-ZrO_2-La_2O_3 supported catalyst. The values compare particularly favourably to those over inert SiO_2 supported Ni that approached 30% below 450°C [25]. As discussed in various studies [46,47] and evidenced by the TPR results, CeO_2 is characterised by its reducibility and ability to provide lattice oxygen species to the metal. These O species can promote the oxidation of CH_x fragments on the metal, while the resulting oxygen vacancies on the support are replenished

by steam. ZrO_2 supported catalyst have also been shown to facilitate steam's dissociation, providing hydroxyl groups to the metal that can similarly promote reforming reactions [48–50]. For both Rh supported catalysts, CH_4 selectivity, within the detection limits of the analytics used, was zero, indicative of the role of the metal in addition to the discussed support effects. Indeed, DFT calculations have shown that on Rh the C-C bond cleavage takes place most likely at the CHCO surface intermediate, in contrast to the more oxophilic Ni where the same scission was predicted to occur mainly at CH_3CO [44]. As a result, with the promotional effect of O or OH species originating from the support, the resulting CH species are oxidised towards CO more efficiently rather than hydrogenating up to CH_4 on Rh in comparison to CH_3 on Ni. Furthermore, as was shown in the work of Angeli et al. during ethane steam reforming [42], the methanation activity of Ni/CeO_2-ZrO_2-La_2O_3 was higher than that over Rh/CeO_2-ZrO_2-La_2O_3, and could potentially further contribute to the observed methane selectivity differences between Ni and Rh catalysts.

The combined promotional effects of metal and support are further demonstrated by the observed CO_x selectivities. CO_2 selectivity (Figure 2b) over both the Ni and Rh catalysts supported on CeO_2-ZrO_2-La_2O_3 is much higher to that obtained over the ZrO_2-La_2O_3 catalysts, especially at the lower temperatures, in very good agreement with the well-recognised high activity of ceria in the water gas shift reaction [51–53]. ZrO_2, on the contrary, as also evidenced from the TPR profiles, has insignificant reducibility. Any oxygen vacancies on ZrO_2 have been shown to originate mainly from metal-support interactions and be much lower in number in comparison to ceria [54]. Clearly, the much higher oxygen mobility of the later is able to drive the oxidation of CO towards CO_2 even at 300°C for both metals, effectively promoting the water gas shift activity. The combined favourable selectivity trends on Rh and on CeO_2-ZrO_2-La_2O_3 in combination with the higher activity obtained are evident on the achieved H_2 yield for that catalyst (Figure 1b).

3.3. *Effect of partial pressure of reactants*

3.3.1. <u>Variation of ethanol partial pressure</u>

The effect of ethanol partial pressure on ESR over Ni and Rh based catalysts is presented in Figure 3. For these experiments the total pressure (1.9 bara), the partial pressure of water (0.74 bara) and GHSV (1.78 s^{-1}) were kept constant, while ethanol's partial pressure was varied from 0.06 bara (S/C = 6 mol_{H_2O} mol_C^{-1}) to 0.37

bara (S/C = 1 mol_{H_2O} mol_C^{-1}). The plots are presented in terms of S/C variation, with the equivalent values of ethanol partial pressure being also annotated. Ethanol conversion and H_2 yield are clearly enhanced with the increase of the S/C ratio (and decrease of ethanol's partial pressure), as this effectively corresponds to a reduction of the ethanol being fed. In line with the discussion in the previous section the CeO_2-ZrO_2-La_2O_3 supported catalysts showed the higher activity in terms of ethanol conversion and H_2 yield, with Rh reaching 95% conversion at the highest S/C, closely followed by Ni at 91% conversion. For the ZrO_2-La_2O_3 supported catalysts the activity was lower but again Rh was better performing than Ni. Various studies have reported Rh based catalysts to have higher activity than Ni for ESR, however the beneficial effects of the ceria support enhance Ni performance reaching an almost comparable level to Rh [55]. Comparison with Ni/SiO_2 [25] is again indicative of this enhancement, with conversion over that catalyst at a S/C of 6 being approximately only 50%. The turnover frequencies (TOF) obtained in these runs as a function of ethanol's partial pressure (Figure 3c) show a positive partial reaction order for ethanol on all catalysts. Consistent with previous works on various catalysts, an ethanol derived surface intermediate is believed to participate in the rate determining step [20,25,56,57], the latter typically suggested to be one of the first dehydrogenation steps [44]. For all catalysts, partial reaction orders smaller than unity are obtained, ranging from 0.16 to 0.35, indicative of a Langmuir-Hinshelwood reaction mechanism being active. For each type of support, the largest TOF values are achieved with the Rh catalysts, in line with the metal's well recognised higher activity in comparison to Ni [58–60], although as discussed the ceria promoting effect leads to the Ni/CeO_2-ZrO_2-La_2O_3 catalyst outperforming the Rh/ZrO_2-La_2O_3.

Figure 4 presents the carbon selectivities of ESR in terms of S/C ratio for these experiments. The observed trends are overall similar for all catalysts, with CO_2 selectivity increasing and those of CH_3CHO and CO decreasing as the S/C ratio increases, in agreement with the expected promotion of reforming and WGS reactions the abundance of steam would incur. In line with the temperature variation experiments, no CH_4 was observed on either of the Rh catalysts, while only small CH_4 amounts were detected on the Ni catalysts at S/C ratios less than 4. Considering that the lowest S/C of 1 tested is sub-stoichiometric for ESR, these results further support that the CH_4 selectivity differences over the two metals are primarily due to the degree of dehydrogenation of the surface species at which C-C cleavage occurs, as discussed above.

Nonetheless, the higher activity of Rh versus Ni in CH_4 steam reforming is also expected to be contributing to observed trends to some degree, particularly at high conversion where evolution of CH_4 in the gas phase is possible [61]. Moreover, the O species from the ceria support enhance clearly the oxidation of formed CH_x surface species on the metal [62], as indicated by the lower CH_4 selectivities obtained on Ni/CeO_2-ZrO_2-La_2O_3 against Ni/ZrO_2-La_2O_3. Support mediated delivery of OH species from ZrO_2 should also be noted, as, over Ni/SiO_2 [25], CH_4 selectivity averaged almost 40% at the same conditions, whereas on Ni/ZrO_2-La_2O_3 it never exceeded 7%. CO_x selectivity profiles for these runs agree with the already discussed trends, with the CO/CO_2 ratio being consistently the lowest over the Rh/CeO_2-ZrO_2-La_2O_3 and the highest over the Ni/ZrO_2-La_2O_3 for all conditions tested.

3.3.2. **Variation of water partial pressure**

The effect of water partial pressure on ESR over Ni and Rh based catalysts is presented in Figure 5. During these experiments the total pressure (1.9 bara), ethanol's partial pressure (0.13 bara) and GHSV (2.36 s^{-1}) were kept constant while varying water's partial pressure from 0.26 bara (S/C = 1 mol_{H_2O} mol_C^{-1}) to 1.56 bara (S/C = 6 mol_{H_2O} mol_C^{-1}). The ethanol conversion is plotted against S/C variation, with the equivalent water partial pressure values being also annotated. In these runs, the rise of the S/C ratio is linearly correlated to the increase of the partial pressure of water. For all the catalysts, ethanol conversion presents a negative trend as water's partial pressure increases, although for the CeO_2-ZrO_2-La_2O_3 supported ones it is milder in comparison to that over the ZrO_2-La_2O_3 ones. This is more noticeable on the TOF plot (Figure 5c), where a clearly negative reaction order in respect to water is obtained for the latter catalysts, whereas on the ceria containing ones the slope is still negative but much closer to zero. Various studies, including our previous work on Ni/SiO_2 [25], have suggested that a negative partial reaction order for steam indicates the competitive adsorption of ethanol and water for the same active sites, with the metal surface being gradually saturated by adsorbed water species [63,64]. Clearly, the high oxygen mobility and large oxygen storage capacity of CeO_2 allows for an efficient dissociation of steam across its entire surface and a fast delivery of O species to the metal that prevents to a large degree the latter's saturation by steam, as carbon-containing surface intermediates are effectively oxidised. On ZrO_2-La_2O_3 supported catalysts, steam adsorbs and dissociates mostly across the metal-support interface, where the oxidation reactions also take place, so the

increase in water's partial pressure potentially impacts in a more pronounced manner the availability of metal active sites [65] resulting in a more negative slope for the water partial reaction order.

The influence of water's partial pressure on the carbon selectivities is shown in Figure 6. Selectivity trends follow those presented on Figure 4 during ethanol partial pressure variation, even though the conversion trend is opposite, indicative of selectivity being mainly driven by the availability of steam derived intermediates [66]. For all the catalysts, increasing water partial pressure enhanced the production of CO_2 at a concurrent decrease of CH_3CHO and CO (and CH_4 where present). CH_4 selectivity again follows previously discussed trends, being effectively zero over the Rh catalysts. For the Ni catalysts much higher CH_4 selectivities are obtained over these runs for S/C$\leq$2 in comparison to the previous section, particularly for the ZrO_2-La_2O_3 supported catalyst. This is most likely linked to the lower partial pressure of water during these experiments ranging from 0.26 to 0.52 bara versus 0.74 bara used previously throughout all conditions and evidences that the availability of OH or O species on the metal depends primarily on the applied partial pressure of water, rather than the effective S/C ratio in the feed. CO_x selectivities similarly follow previously discussed trends, with the CeO_2-ZrO_2-La_2O_3 supported catalysts showing again the best performance in terms of promoting the WGS reaction through the oxidation of CO by ceria delivered O species. At the highest water partial pressure and S/C tested, the selectivity to CO_2 both for the Ni and Rh on CeO_2-ZrO_2-La_2O_3 catalysts is approximately 95%. The CO/CO_2 ratio in the product gas is for both catalysts equal to 0.05, comparing well with the thermodynamically predicted value of 0.02, and indicating that the water gas shift reaction has approached equilibrium. In combination with the high conversions achieved at these conditions, maximum hydrogen production is obtained.

The selectivity of CH_3CHO is seen to decrease while increasing the water partial pressure, possibly linked and discussed in more detail by Zhurka et al. to the ethanol conversion trend [25]. CH_3CHO is a primary product of ESR, derived from ethanol's dehydrogenation, and, as such, its formation should be independent of steam derived species. In these experiments the partial pressure of ethanol is kept constant while increasing the water partial pressure, leading to a saturation of the metal surface and a drop in ethanol conversion and, as such, in the production of CH_3CHO. As commented on previous sections, an alternate pathway through

acetaldehyde's oxidation by O species to acetate species, the latter decomposing to CH_x and CO_x, is possible [67] and could link to the lower CH_3CHO selectivity on CeO_2-ZrO_2-La_2O_3 supported catalysts. Nonetheless, as discussed, this is believed to be a relatively minor contribution to the overall results obtained.

Overall, H_2 yield (Figure 5b) remains relatively constant with water partial pressure, even though conversion decreases for all catalysts due to the beneficial selectivities brought about by the excess of water. Specifically, a slightly decreasing trend is observed for Rh, while for Ni, the mild variation of the values lies within the experimental error, so no clear trend can be discerned. Comparatively, the difference between the two metals can be attributed to the substantial drop in CH_4 selectivity attained with S/C increase on the Ni catalysts.

3.4. *Effect of space time*

The effect of space time on ethanol conversion and H_2 yield at 400°C and S/C = 3 is presented in Figure 7. The space time was varied from 69.80 to 348.98 g_{cat} s g_{Eth}^{-1} by changing the reactants flow over a fixed mass of catalyst. As expected, ethanol conversion increases with space time, with the H_2 yield following this trend. The higher activity of the CeO_2-ZrO_2-La_2O_3 supported catalysts on conversion is evident, which translates to these two catalysts achieving remarkably higher H_2 yields at the higher space times tested in comparison to the ZrO_2-La_2O_3 supported catalysts. At a space time of 348.98 g_{cat} s g_{Eth}^{-1} conversion over both the CeO_2-ZrO_2-La_2O_3 supported catalysts exceeded 80% with H_2 yield being 75 and 83% of the stoichiometrically possible for Ni and Rh, respectively. Conversion and H_2 yield over ZrO_2-La_2O_3 supported catalysts reached 61 and 47%, and 67 and 61%, for Ni and Rh respectively. For both supports, though, and in line with discussions in previous sections, Rh consistently performed better to its equivalent Ni catalyst, whereas the worse performing Ni catalyst (supported on ZrO_2-La_2O_3) still showed marginally higher conversion to Ni/SiO_2 (discussed elsewhere [25]). At the largest space velocity tested (GHSV = 3.89 s^{-1}, $W/F_{Eth,t0}$ = 69.80 g_{cat} s g_{Eth}^{-1}), TOF values obtained ranged from 2.76 s^{-1} and 3.04 s^{-1} for the Ni and Rh on ZrO_2-La_2O_3 to 4.37 s^{-1} and 6.33 s^{-1} for the Ni and Rh on CeO_2-ZrO_2-La_2O_3. Rh showed higher activity than Ni for each support, however the presence of ceria allows for higher turnover frequencies to be attained on Ni versus the non-ceria containing Rh sample, which evidences its substantial promoting effect on the reaction kinetics. Notwithstanding the difficulties in

comparing turnover frequencies with literature given the differences in conditions and supports employed and the overall high conversions in this work, Table S3 in the Supporting Information provides a summary of values reported in literature for Ni and Rh catalysts with those in the current work. Those obtained on Ni catalysts compare well with published, e.g. as summarised in Kubacka et al. [68] and Chen et al. [69], as most reported do not exceed 1 s^{-1}. On Rh TOF values in the order of 10 s^{-1} have been reported [39,70], but, accounting again for the variable conditions, etc. these have been obtained at, the current results appear competitive.

Figure 8 presents the product selectivities plotted against ethanol conversion, whereas Figure S3 in the Supporting Information provides the selectivity trends against space time. The conversions achieved over these space time variation runs, particularly for the CeO_2-ZrO_2-La_2O_3 supported catalysts are higher than what would typically allow a kinetic evaluation of the reaction pathway and the identification of primary and secondary products. Nonetheless, the comparison of obtained performances reveals noteworthy trends that can be linked to the underlying pathway. The selectivity of CH_3CHO evolves similarly over all catalysts, namely decreasing up to a value of zero with the increase of space time, in agreement with acetaldehyde being a primary product of ESR over both Rh and Ni resulting from ethanol's dehydrogenation [31,43]. The very similar selectivity values for all catalysts at each conversion level further support that the formation of acetaldehyde is primarily metal driven and not affected by the availability of steam derived intermediates.

CH_4 selectivity, interestingly, exhibits diverging profiles at the studied conditions. For the Rh catalysts, as consistently observed in all experiments of this work, no CH_4 production was observed, consolidating our observations on the role of Rh in promoting the dehydrogenation of surface intermediates, prior the cleavage of the C-C bond. On the Ni/ZrO_2-La_2O_3, CH_4 selectivity is seen to increase with space time, a trend consistent with methane being identified as a secondary product of ESR [25]. For the Ni/CeO_2-ZrO_2-La_2O_3 catalyst, though, CH_4 selectivity is observed to decrease as space time increases, which would imply CH_4 is a primary product over this catalyst. Nonetheless, this trend is attributed to the high conversions in these experiments and the abundance of reactive O species from the support that lead to an effective oxidation of CH_x species. It would most probably require measurements at much lower conversions for CH_4 to be able to be identified

as a secondary product for this catalyst. In all cases, the considerably lower selectivities for CH_4 obtained over these catalysts in comparison to Ni/SiO_2 [25] needs to be highlighted. At the highest conversion achieved over the silica supported catalyst (60%), CH_4 selectivity was as high as 35%, while for the current catalysts it ranged from 6 to 0% depending on the metal and support.

The above observation is consistent also with the obtained CO_x selectivities in these experiments. CO selectivity over both ZrO_2-La_2O_3 catalysts increases gradually with space time, while the opposite trend is seen over the CeO_2-ZrO_2-La_2O_3 catalysts. Even though for Rh it has been discussed based on DFT calculations that CHCO formation, leading eventually to CO, can take place also via surface pathways that do not involve CH_3CHO [44], for Ni and the low temperature tested this is considered less likely. In our previous work it was discussed both based on experimental results [25] and via microkinetic modelling [64] that even over Ni/SiO_2 it is possible that a primary pathway towards the formation of CO can exist, but that was shown to be primarily active only at temperatures over 500°C. Considering the opposite CO trends over the ZrO_2-La_2O_3 supported catalysts, it is believed that it is the high oxygen mobility of the ceria, leading to a very efficient oxidation of CO over these catalysts, that results in CO appearing as a primary product. The decisive role of the ceria support in promoting secondary CO conversion reactions is further evident by the almost identical CO selectivities over the two CeO_2-ZrO_2-La_2O_3 catalysts across the range of conversions studied. At the highest conversion achieved, a CO/CO_2 ratio of 0.04 and 0.09 on Rh and Ni, respectively, approached the thermodynamically predicted value of 0.02, indicative again of the water gas shift reaction being almost quasi-equilibrated. Over the ZrO_2-La_2O_3 catalysts the lower activity and participation of the support in the reaction mechanism allows for the role of the metal to become more evident with Rh seen to outperform Ni. CO_2 selectivity, finally, displays a rising trend for all catalysts, although more pronounced over the CeO_2-ZrO_2-La_2O_3 catalysts, that agrees with CO_2 being a secondary product from the, primarily support-mediated, oxidation of CO. The comparison with Ni/SiO_2 [25] is again revealing of the much higher performance of the current catalysts. A very high CO_2 selectivity of 85% was achieved over both Ni and Rh CeO_2-ZrO_2-La_2O_3 supported catalysts at a conversion of 60%, whereas for Ni/SiO_2 the same metric did not exceed 25% at this conversion. The ZrO_2-La_2O_3 catalysts performed still favourably to Ni/SiO_2 with CO_2 selectivities of 70 and 47% for Rh and Ni, respectively.

3.5. *Time-on-stream performance*

Figure 9 presents the evolution of ethanol conversion and H_2 yield with time, to investigate the stability of the catalysts at 500°C and S/C = 3 (GHSV = 1.08 s^{-1}), conditions where thermodynamic equilibrium predicts the conversion of ethanol to be complete. For all catalysts, an overall stable behaviour was observed regarding the conversion and H_2 yield for the duration of 240 min tested. The CeO_2-ZrO_2-La_2O_3 supported catalysts exhibited much higher performance, almost approaching equilibrium, with conversion averaging 90% for Ni and over 95% for Rh. ZrO_2-La_2O_3 supported catalysts were less active with respective conversions of approximately 60% and 70% for Ni and Rh being measured. Moreover, these catalysts appeared to deactivate slowly with time, with the gradual decrease in conversion and H_2 yield being more evident on the Ni catalyst. The same catalysts, when used in simulated biogas steam reforming at very similar conditions of 500°C temperature and S/C = 3, showed analogous behaviour with again the CeO_2-ZrO_2-La_2O_3 supported catalysts being the most stable over extended time-on-stream experiments of up to 90 h [37]. Clearly, the oxygen species delivered by ceria contribute actively to the oxidation of coke precursors and any formed carbonaceous deposits. Moreover, as all catalysts have been exposed to a temperature of 500°C during their reduction prior each experiment, sintering is considered less likely to be the main cause for the observed slow deactivation of the ZrO_2-La_2O_3 supported catalysts.

The evolution of total carbon selectivities with time-on-stream is presented in Figure 10. Acetaldehyde's selectivity is very low at roughly 2 and 1% for the ZrO_2-La_2O_3 and CeO_2-ZrO_2-La_2O_3 supported catalysts, respectively, and very stable over time, indicating that the main activation pathway of ethanol proceeds unhindered over all catalysts. Interestingly, there was no CH_4 detected over any of the catalysts for the duration of these time-on-stream experiments. It appears that at the conditions tested of high operating temperature and relatively large space time the beneficial effects of the supports are able to supress completely the formation of CH_4, not only for the Rh catalysts, but also on Ni. This can further be observed from the very high CO_2 selectivity which surpassed 90% on all catalysts, reaching as high as 95% on the CeO_2-ZrO_2-La_2O_3 supported ones. Evidently, at this high temperature the O and OH species that spillover from the supports are abundant enough to effectively promote the water gas shift reaction. Nonetheless, a gradual

increase of CO selectivity at the expense of CO_2 is observed with time, mainly on the ZrO_2-La_2O_3 supported catalysts, indicating that the slow catalyst deactivation impacts first on the water gas shift reaction progression [25,29]. This effect is rather minor with the overall performance, particularly on the CeO_2-ZrO_2-La_2O_3 supported catalysts being very stable resulting in high H_2 yield at high conversions. For the most active catalyst, the Rh/CeO_2-ZrO_2-La_2O_3 a very high H_2 yield of approximately 90% of the stoichiometrically possible was achieved and remained constant for the duration of these TOS runs, indicative of the potential of this catalyst for ESR.

3.6. *Temperature-programmed oxidation of spent catalysts*

Carbon deposits on the spend catalysts, collected after the TOS experiments, were characterized via TPO. The CO_2 evolution profiles for the four catalysts are presented in Figure 11, while Table 1 presents the amount of carbon deposited on the catalyst bed in terms of catalyst weight mass and carbon fed. Two peaks are visible on the TPO profiles of Ni catalysts suggesting the existence of carbon deposits of different nature on both catalysts. Specifically, the Ni/ZrO_2-La_2O_3 catalyst showed an intense peak at 503^{o}C and a broader peak at 611^{o}C, while on Ni/CeO_2-ZrO_2-La_2O_3 lower in magnitude peaks were observed at 491^{o}C and 610^{o}C. The peaks around 500^{o}C could be attributed to amorphous carbon produced through polymerization reactions, while those around 610^{o}C would suggest the formation of filamentous or whisker carbon [71]. The different types of coke deposited on Ni during steam reforming of various compounds have been widely reported [72,73], suggesting amorphous carbon, covering active sites, to result in catalytic activity decrease, while filamentous carbon, diffusing through Ni and leaving active sites still accessible, to not lead to pronounced deactivation [74]. The overall higher amount of coke deposited, particularly of amorphous carbon, on Ni/ZrO_2-La_2O_3 is in agreement with the TOS results where that catalyst was shown to exhibit a relatively higher deactivation compared to Ni/CeO_2-ZrO_2-La_2O_3. Correspondingly, the high and stable performance of Ni/CeO_2-ZrO_2-La_2O_3 and the graphitic nature of coke formed has been previously reported by Vagia et al. [75] examining acetic acid steam reforming. On the CeO_2-ZrO_2-La_2O_3 supported Ni catalyst only 0.25% of the carbon fed was deposited as coke after the 4 h TOS run, comparing favorably to 0.63% on the ZrO_2-La_2O_3

supported catalyst, both values being particularly lower to the approximately 3% measured after equivalent experiments over Ni/SiO_2 [25].

Rh based catalysts presented only one minor peak and exhibited clearly lower carbon formation in relation to the Ni catalysts, agreeing well with their overall higher catalytic activity and stability. Rh/ZrO_2-La_2O_3 catalyst showed a low CO_2 peak at 626°C during TPO indicating the presence of filamentous carbon. The displacement of the TPO peak on Rh/ZrO_2-La_2O_3 at higher oxidizing temperature in comparison to Ni/ZrO_2-La_2O_3 aligns well with the findings of Chiodo et al. during glycerol steam reforming [76] and Angeli et al. during methane steam reforming [37], who both observed filamentous coke on Rh being slightly more difficult to oxidize than on Ni. Considering the very low amounts of coke on Rh/ZrO_2-La_2O_3 (0.09% of carbon fed) in comparison to both Ni samples, the slight deactivation on this catalyst could indicate the possibility of a gradual change in the oxidation state of Rh, in line with the discussion by Angeli et al. [37]. On Rh/CeO_2-ZrO_2-La_2O_3 only a very minor peak was detected, amounting a minimal carbon deposition of 0.01% of carbon fed, underlining again the synergetic effect of the noble metal and the ceria support. The high catalytic activity and coke resistance of Rh/CeO_2-ZrO_2-La_2O_3 on methane, ethane and propane steam reforming has been examined by Angeli et al. [42] presenting always low intensity TPO profiles with nearly no carbon formation.

Conclusively, CeO_2-ZrO_2-La_2O_3 supported catalysts exhibited higher coke resistance and lower carbon formation in comparison to the respective ZrO_2-La_2O_3 supported catalysts, due to ceria's OSC and increased oxygen mobility which participated in the oxidation of carbon precursors and deposits. Regarding the active metal, Rh catalysts showed lower carbon formation due to their high resistance towards carbon formation. Overall, the Rh/CeO_2-ZrO_2-La_2O_3 catalyst displayed the best catalytic performance with minor carbon formation.

4. Conclusions

In this study the catalytic activity of Ni and Rh based catalysts supported over (CeO_2)-ZrO_2-La_2O_3 mixed oxides was examined, focusing on discriminating the effect of the metal and the support on the ESR reaction. All

catalysts showed higher activity compared to Ni/SiO_2, on account of the ability of ZrO_2 to promote the dissociation of water and supply OH species to the metal, as evidenced by both the higher conversions and favourable selectivities obtained. CeO_2 containing catalysts were clearly the most active due to ceria's high oxygen mobility that enhanced oxidation reactions, particularly of CO towards CO_2, effectively promoting the water gas shift reaction. Furthermore, CeO_2 enhanced the coke resistance of the catalysts, demonstrated during stability runs and via TPO analysis of spent samples. Rh based catalysts were respectively the most active with noteworthy being the absence of CH_4 in the products even at low contact time. This was attributed to the Rh metal favouring the dehydrogenation reactions over the C-C bond cleavage, resulting in highly dehydrogenated surface species that can be effectively oxidised. The latter characteristic further contributed to the coke resistance of Rh versus Ni catalysts, shown in the minimal coke deposits measured. The combined support and metal effects resulted in Rh/CeO_2-ZrO_2-La_2O_3 exhibiting the highest performance and stability, closely followed by Ni/CeO_2-ZrO_2-La_2O_3.

CRediT author statement

Marinela D. Zhurka: Investigation, Writing - Original Draft. **Angeliki A. Lemonidou:** Resources, Writing - Review & Editing. **Panagiotis N. Kechagiopoulos:** Conceptualization, Methodology, Writing - Review & Editing, Supervision.

Declaration of interests

The authors declare that they have no known competing financial interests or personal relationships that could have appeared to influence the work reported in this paper.

Acknowledgments

We thank Dr Alan McCue from the Department of Chemistry, University of Aberdeen, for assisting in carrying out the TPO measurements.

References

[1] F. Martins, C. Felgueiras, M. Smitkova, N. Caetano, Analysis of fossil fuel energy consumption and environmental impacts in european countries, Energies. 12 (2019) 1–11.

[2] L. Xu, Y. Wang, S.A.A. Shah, H. Zameer, Y.A. Solangi, G. Das Walasai, Z.A. Siyal, Economic Viability and Environmental Efficiency Analysis of Hydrogen Production Processes for the Decarbonization of Energy Systems, Processes. 7 (2019) 494.

[3] B. Dou, H. Zhang, Y. Song, L. Zhao, B. Jiang, M. He, C. Ruan, H. Chen, Y. Xu, Hydrogen production from the thermochemical conversion of biomass: Issues and challenges, Sustain. Energy Fuels. 3 (2019) 314–342.

[4] P. Manzanares, Bioalcohol Production: Biochemical Conversion of Lignocellulosic Biomass, 2010.

[5] L.C. Chen, S.D. Lin, The ethanol steam reforming over Cu-Ni/SiO_2 catalysts: Effect of Cu/Ni ratio, Appl. Catal. B Environ. 106 (2011) 639–649.

[6] L.P.R. Profeti, E.A. Ticianelli, E.M. Assaf, Production of hydrogen by ethanol steam reforming on Co/Al_2O_3 catalysts: Effect of addition of small quantities of noble metals, J. Power Sources. 175 (2008) 482–489.

[7] D.K. Liguras, D.I. Kondarides, X.E. Verykios, Production of hydrogen for fuel cells by steam reforming of ethanol over supported noble metal catalysts, Appl. Catal. B Environ. 43 (2003) 345–354.

[8] M. Benito, R. Padilla, L. Rodríguez, J.L. Sanz, L. Daza, Zirconia supported catalysts for bioethanol steam reforming: Effect of active phase and zirconia structure, J. Power Sources. 169 (2007) 167–176.

[9] B. Valle, B. Aramburu, A. Remiro, J. Bilbao, A.G. Gayubo, Effect of calcination/reduction conditions of Ni/La_2O_3-αAl_2O_3 catalyst on its activity and stability for hydrogen production by steam reforming of raw bio-oil/ethanol, Appl. Catal. B Environ. 147 (2014) 402–410.

[10] A. Ochoa, B. Aramburu, B. Valle, D.E. Resasco, J. Bilbao, A.G. Gayubo, P. Castaño, Role of oxygenates and effect of operating conditions in the deactivation of a Ni supported catalyst during the steam reforming of bio-oil, Green Chem. 19 (2017) 4315–4333.

[11] A. Iulianelli, S. Liguori, T. Longo, S. Tosti, P. Pinacci, A. Basile, An experimental study on bio-ethanol steam reforming in a catalytic membrane reactor. Part II: Reaction pressure, sweep factor and WHSV effects, Int. J. Hydrogen Energy. 35 (2010) 3159–3164.

[12] Y. Chandra, A. Kumar, R. Prasad, S. Nath, Ethanol steam reforming for hydrogen production : Latest and effective catalyst modification strategies to minimize carbonaceous deactivation, Renew. Sustain. Energy Rev. 74 (2017) 89–103.

[13] K.D. Punase, N. Rao, P. Vijay, A review on mechanistic kinetic models of ethanol steam reforming for hydrogen production using a fixed bed reactor, Chem. Pap. 73 (2019) 1027–1042.

[14] C. Montero, A. Remiro, P.L. Benito, J. Bilbao, A.G. Gayubo, Optimum operating conditions in ethanol steam reforming over a Ni/La_2O_3-αAl_2O_3 catalyst in a fluidized bed reactor, Fuel Process. Technol. 169 (2018) 207–216.

[15] A. Kumar, R. Prasad, Y.C. Sharma, Ethanol steam reforming with Co^0 (111) for hydrogen and carbon nanofilament generation, Resour. Technol. 3 (2017) 422–428.

[16] F.A. da Silva, I. Dancini-Pontes, M. DeSouza, N.R.C. Fernandes, Kinetics of ethanol steam reforming over Cu–Ni/Nb_xO_y catalyst, React. Kinet. Mech. Catal. 122 (2017) 557–574.

[17] D.R. Sahoo, S. Vajpai, S. Patel, K.K. Pant, Kinetic modeling of steam reforming of ethanol for the production of hydrogen over Co/Al_2O_3 catalyst, Chem. Eng. J. 125 (2007) 139–147.

[18] C. Graschinsky, M. Laborde, N. Amadeo, A. Le Valant, N. Bion, F. Epron, D. Duprez, Ethanol steam reforming over $Rh(1\%)MgAl_2O_4/Al_2O_3$: A kinetic study, Ind. Eng. Chem. Res. 49 (2010) 12383–12389.

[19] F. Wang, W. Cai, C. Descorme, H. Provendier, W. Shen, C. Mirodatos, Y. Schuurman, From mechanistic to kinetic analyses of ethanol steam reforming over Ir/CeO_2 catalyst, Int. J. Hydrogen Energy. 39 (2014) 18005–18015.

[20] P.D. Vaidya, A.E. Rodrigues, Kinetics of steam reforming of ethanol over a Ru/Al_2O_3 catalyst, Ind. Eng. Chem. Res. 45 (2006) 6614–6618.

[21] M. Cobo, D. Pieruccini, R. Abello, L. Ariza, L.F. Córdoba, J.A. Conesa, Steam reforming of ethanol over bimetallic $RhPt/La_2O_3$: Long-term stability under favorable reaction conditions, Int. J. Hydrogen Energy. 38 (2013) 5580–5593.

[22] A.M. da Silva, K.R. de Souza, G. Jacobs, U.M. Graham, B.H. Davis, L. V. Mattos, F.B. Noronha, Steam and CO_2 reforming of ethanol over Rh/CeO_2 catalyst, Appl. Catal. B Environ. 102 (2011) 94–109.

[23] J. Zhang, Z. Zhong, P. Hu, M.B. Sullivan, L. Chen, Ethanol Steam Reforming on Rh Catalysts: Theoretical and Experimental Understanding, ACS Catal. 4 (2013) 448–456.

[24] A.A. Lemonidou, E.C. Vagia, J.A. Lercher, Acetic Acid Reforming over Rh Supported on La_2O_3/CeO_2–ZrO_2: Catalytic Performance and Reaction Pathway Analysis, ACS Catal. 3 (2013) 1919–1928.

[25] M.D. Zhurka, A.A. Lemonidou, J.A. Anderson, P.N. Kechagiopoulos, Kinetic analysis of the steam reforming of ethanol over Ni/SiO_2 for the elucidation of metal-dominated reaction pathways, React. Chem. Eng. 3 (2018) 883–897.

[26] I. Llera, V. Mas, M.L. Bergamini, M. Laborde, N. Amadeo, Bio-ethanol steam reforming on Ni based catalyst. Kinetic study, Chem. Eng. Sci. 71 (2012) 356–366.

[27] C. Zhang, S. Li, G. Wu, Z. Huang, Z. Han, T. Wang, J. Gong, Steam reforming of ethanol over skeletal Ni-based catalysts: A temperature programmed desorption and kinetic study, AIChE J. 60 (2014) 635–644.

[28] T.K. Phung, G. Busca, Diethyl ether cracking and ethanol dehydration: Acid catalysis and reaction paths, Chem. Eng. J. 272 (2015) 92–101.

[29] C. Montero, A. Remiro, B. Valle, L. Oar-Arteta, J. Bilbao, A.G. Gayubo, Origin and Nature of Coke in Ethanol Steam Reforming and Its Role in Deactivation of Ni/La_2O_3-αAl_2O_3 Catalyst, Ind. Eng. Chem. Res. 58 (2019) 14736–14751.

[30] S.M. Gates, J.N. Russell, J.T. Yates, Bond activation sequence observed in the chemisorption and surface reaction of ethanol on Ni(111), Surf. Sci. 171 (1986) 111–134.

[31] M.A. Ebiad, D.R. Abd El-Hafiz, R.A. Elsalamony, L.S. Mohamed, Ni supported high surface area CeO_2-ZrO_2 catalysts for hydrogen production from ethanol steam reforming, RSC Adv. 2 (2012) 8145–8156.

[32] W. Sutthisripok, S. Sattayanurak, L. Sikong, Effect of specific surface area on oxygen storage capacity (OSC) and methane steam reforming reactivity of CeO_2, J. Porous Mater. 15 (2008) 519–525.

[33] W. Xu, Z. Liu, A.C. Johnston-Peck, S.D. Senanayake, G. Zhou, D. Stacchiola, E.A. Stach, J.A. Rodriguez, Steam reforming of ethanol on Ni/CeO_2: Reaction pathway and interaction between Ni and the CeO_2 support, ACS Catal. 3 (2013) 975–984.

[34] Y. Matsumura, T. Nakamori, Steam reforming of methane over nickel catalysts at low reaction

temperature, Appl. Catal. A Gen. 258 (2004) 107–114.

[35] J.Y. Liu, W.N. Su, J. Rick, S.C. Yang, C.J. Pan, J.F. Lee, J.M. Chen, B.J. Hwang, Rational design of ethanol steam reforming catalyst based on analysis of Ni/La_2O_3 metal-support interactions, Catal. Sci. Technol. 6 (2016) 3449–3456.

[36] A.N. Fatsikostas, D.I. Kondarides, X.E. Verykios, Production of hydrogen for fuel cells by reformation of biomass-derived ethanol, 75 (2002) 145–155.

[37] S.D. Angeli, L. Turchetti, G. Monteleone, A.A. Lemonidou, Catalyst development for steam reforming of methane and model biogas at low temperature, Appl. Catal. B Environ. 181 (2016) 34–46.

[38] J.F. Da Costa-Serra, R. Guil-López, A. Chica, Co/ZnO and Ni/ZnO catalysts for hydrogen production by bioethanol steam reforming. Influence of ZnO support morphology on the catalytic properties of Co and Ni active phases, Int. J. Hydrogen Energy. 35 (2010) 6709–6716.

[39] N. Palmeri, S. Cavallaro, V. Chiodo, S. Freni, F. Frusteri, J.C.J. Bart, Hydrogen production from ethanol on Rh/MgO based catalysts. The influence of rhodium precursor on catalytic performance, Int. J. Hydrogen Energy. 32 (2007) 3335–3342.

[40] S. Wang, W. Guo, L. Guo, X. Li, Q. Wang, Experimental and subsequent mechanism research on the steam reforming of ethanol over a Ni/CeO_2 catalyst, Int. J. Green Energy. 12 (2015) 694–701.

[41] M. Patel, T.K. Jindal, K.K. Pant, Kinetic Study of Steam Reforming of Ethanol on Ni-Based Ceria – Zirconia Catalyst, Ind. Eng. Chem. Res. 52 (2013) 15763–15771.

[42] S.D. Angeli, F.G. Pilitsis, A.A. Lemonidou, Methane steam reforming at low temperature : Effect of light alkanes' presence on coke formation, Catal. Today. 242 (2015) 119–128.

[43] A. Yee, S.. Morrison, H. Idriss, The reactions of ethanol over M/CeO_2 catalysts, Catal. Today. 63 (2000) 327–335.

[44] J.E. Sutton, D.G. Vlachos, Ethanol Activation on Closed-Packed Surfaces, Ind. Eng. Chem. Res. 54 (2015) 4213–4225.

[45] A. Gazsi, A. Koós, T. Bánsági, F. Solymosi, Adsorption and decomposition of ethanol on supported Au catalysts, Catal. Today. 160 (2011) 70–78.

[46] N. Laosiripojana, W. Sutthisripok, S. Assabumrungrat, Reactivity of high surface area CeO_2 synthesized by surfactant-assisted method to ethanol decomposition with and without steam, Chem. Eng. J. 127 (2007) 31–38.

[47] H. Song, X. Bao, C.M. Hadad, Adsorption/Desorption Behavior of Ethanol Steam Reforming Reactants and Intermediates over Supported Cobalt Catalysts, Catal. Letters. 141 (2011) 43–54.

[48] S. Li, M. Li, C. Zhang, S. Wang, X. Ma, J. Gong, Steam reforming of ethanol over Ni/ZrO_2 catalysts: Effect of support on product distribution, Int. J. Hydrogen Energy. 37 (2012) 2940–2949.

[49] F. Pompeo, N.N. Nichio, M.M.V.M. Souza, D. V Cesar, O.A. Ferretti, M. Schmal, Study of Ni and Pt catalysts supported on α-Al_2O_3 and ZrO_2 applied in methane reforming with CO_2, Appl. Catal. A Gen. 316 (2007) 175–183.

[50] Charisiou N. D., K.N. Papageridis, G. Siakavelas, L. Tzounis, K. Kousi, M.A. Baker, S.J. Hinder4, V. Sebastian, K. Polychronopoulou, A.M. Goula, Glycerol Steam Reforming for Hydrogen Production over Nickel Supported on Alumina, Zirconia and Silica Catalysts, Top. Catal. 60 (2017) 1226–1250.

[51] D. Carta, T. Montini, M.F. Casula, M. Monai, S. Bullita, P. Fornasiero, A. Corrias, The water gas shift reaction over Pt–CeO_2 nanoparticles confined within mesoporous SBA-16, J. Mater. Chem. A. 5 (2017)

20024–20034.

[52] E.T. Saw, U. Oemar, M.L. Ang, H. Kus, S. Kawi, High-temperature water gas shift reaction on Ni-Cu/CeO_2 catalysts: effect of ceria nanocrystal size on carboxylate formation, Catal. Sci. Technol. 6 (2016) 5336–5349.

[53] C. Chen, Y. Zhan, J. Zhou, D. Li, Y. Zhang, X. Lin, L. Jiang, Q. Zheng, Cu/CeO_2 Catalyst for Water-Gas Shift Reaction: Effect of CeO_2 Pretreatment, ChemPhysChem. 19 (2018) 1448–1455.

[54] H. Song, U.S. Ozkan, Ethanol steam reforming over Co-based catalysts: Role of oxygen mobility, J. Catal. 261 (2009) 66–74.

[55] J.L. Contreras, J. Salmones, J.A. Colín-Luna, L. Nuño, B. Quintana, I. Córdova, B. Zeifert, C. Tapia, G.A. Fuentes, Catalysts for H_2 production using the ethanol steam reforming (a review), Int. J. Hydrogen Energy. 39 (2014) 18835–18853.

[56] P.J. Lu, T.S. Chen, J.M. Chern, Reaction network and kinetic analysis of ethanol steam reforming over a Ru/Al_2O_3 catalyst, in: Catal. Today, Elsevier B.V., 2011: pp. 17–24.

[57] M. Patel, T.K. Jindal, K.K. Pant, Kinetic study of steam reforming of ethanol on Ni-based ceria-zirconia catalyst, Ind. Eng. Chem. Res. 52 (2013) 15763–15771.

[58] M. Zeppieri, P.L. Villa, N. Verdone, M. Scarsella, P. De Filippis, Kinetic of methane steam reforming reaction over nickel- and rhodium-based catalysts, Appl. Catal. A Gen. 387 (2010) 147–154.

[59] J.R. Rostrup-Nielsen, J.H. Bak Hansen, CO_2-reforming of methane over transition metals, J. Catal. 144 (1993) 38–49.

[60] N. Bion, F. Epron, D. Duprez, Bioethanol reforming for H_2 production. A comparison with hydrocarbon reforming, 2010.

[61] S. Lee, Methane and its Derivatives, Taylor & Francis, 1996.

[62] Z. Liu, S.D. Senanayake, J.A. Rodriguez, Environmental Elucidating the interaction between Ni and CeO x in ethanol steam reforming catalysts : A perspective of recent studies over model and powder systems, Appl. Catal. B, Environ. 197 (2016) 184–197.

[63] G. Zeng, Y. Li, U. Olsbye, Kinetic and process study of ethanol steam reforming over Ni/Mg(Al)O catalysts: The initial steps, Catal. Today. 259 (2015) 312–322.

[64] F. Tijani Ahmed Afolabi, C. Li, P.N. Kechagiopoulos, Microkinetic modelling and reaction pathway analysis of the steam reforming of ethanol over Ni/SiO_2, Int. J. Hydrogen Energy. 44 (2019) 22816–22830.

[65] M.M. Kauppinen, M.M. Melander, A.S. Bazhenov, K. Honkala, Unraveling the Role of the Rh–ZrO_2 Interface in the Water–Gas-Shift Reaction via a First-Principles Microkinetic Study, ACS Catal. 8 (2018) 11633–11647.

[66] J.E. Sutton, P. Panagiotopoulou, X.E. Verykios, D.G. Vlachos, Combined DFT, Microkinetic, and Experimental Study of Ethanol Steam Reforming on Pt, J. Phys. Chem. C. 117 (2013) 4691–4706.

[67] B.H. Idriss, Ethanol Reactions over the Surfaces of Noble Metal/Cerium Oxide Catalysts, Platin. Met. Rev. 48 (2004) 105–115.

[68] A. Kubacka, M. Fernández-García, A. Martínez-Arias, Catalytic hydrogen production through WGS or steam reforming of alcohols over Cu, Ni and Co catalysts, Appl. Catal. A Gen. 518 (2016) 2–17.

[69] L.C. Chen, S.D. Lin, Effects of the pretreatment of CuNi/SiO_2 on ethanol steam reforming: Influence of

bimetal morphology, Appl. Catal. B Environ. 148–149 (2014) 509–519.

[70] F. Frusteri, S. Freni, L. Spadaro, V. Chiodo, G. Bonura, S. Donato, S. Cavallaro, H2 production for MC fuel cell by steam reforming of ethanol over MgO supported Pd, Rh, Ni and Co catalysts, Catal. Commun. 5 (2004) 611–615.

[71] C. V. Satyanarayana, D. Srikant, H.R. Gurav, Industrial Catalytic Processes for Fine and Specialty Chemicals, Elsevier Inc., 2016.

[72] L. He, S. Hu, L. Jiang, S.S.A. Syed-Hassan, Y. Wang, K. Xu, S. Su, J. Xiang, L. Xiao, H. Chi, X. Chen, Opposite effects of self-growth amorphous carbon and carbon nanotubes on the reforming of toluene with Ni/A-Al_2O_3 for hydrogen production, Int. J. Hydrogen Energy. 42 (2017) 14439–14448.

[73] M.D.M.V.M. Souza, L. Clavé, V. Dubois, C.A.C. Perez, M. Schmal, Activation of supported nickel catalysts for carbon dioxide reforming of methane, Appl. Catal. A Gen. 272 (2004) 133–139.

[74] J.W. Snoeck, G.F. Froment, M. Fowles, Filamentous carbon formation and gasification: Thermodynamics, driving force, nucleation, and steady-state growth, J. Catal. 169 (1997) 240–249.

[75] E.C. Vagia, A.A. Lemonidou, Investigations on the properties of ceria-zirconia-supported Ni and Rh catalysts and their performance in acetic acid steam reforming, J. Catal. 269 (2010) 388–396.

[76] V. Chiodo, S. Freni, A. Galvagno, N. Mondello, F. Frusteri, Catalytic features of Rh and Ni supported catalysts in the steam reforming of glycerol to produce hydrogen, Appl. Catal. A Gen. 381 (2010) 1–7.

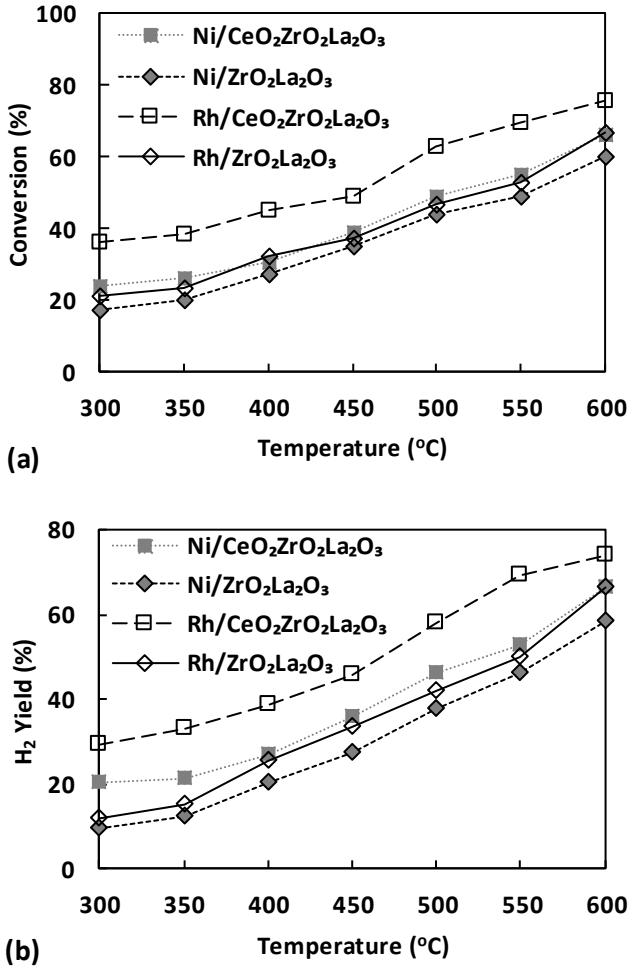

Figure 1. Temperature effect on ethanol conversion (a) and H_2 yield (b) over Ni and Rh based catalysts supported on (CeO_2)-ZrO_2-La_2O_3 ($W/F_{Eth,t_0}$ = 91.88 g_{cat} s g_{Eth}^{-1}, P = 1.7 bara, S/C = 3).

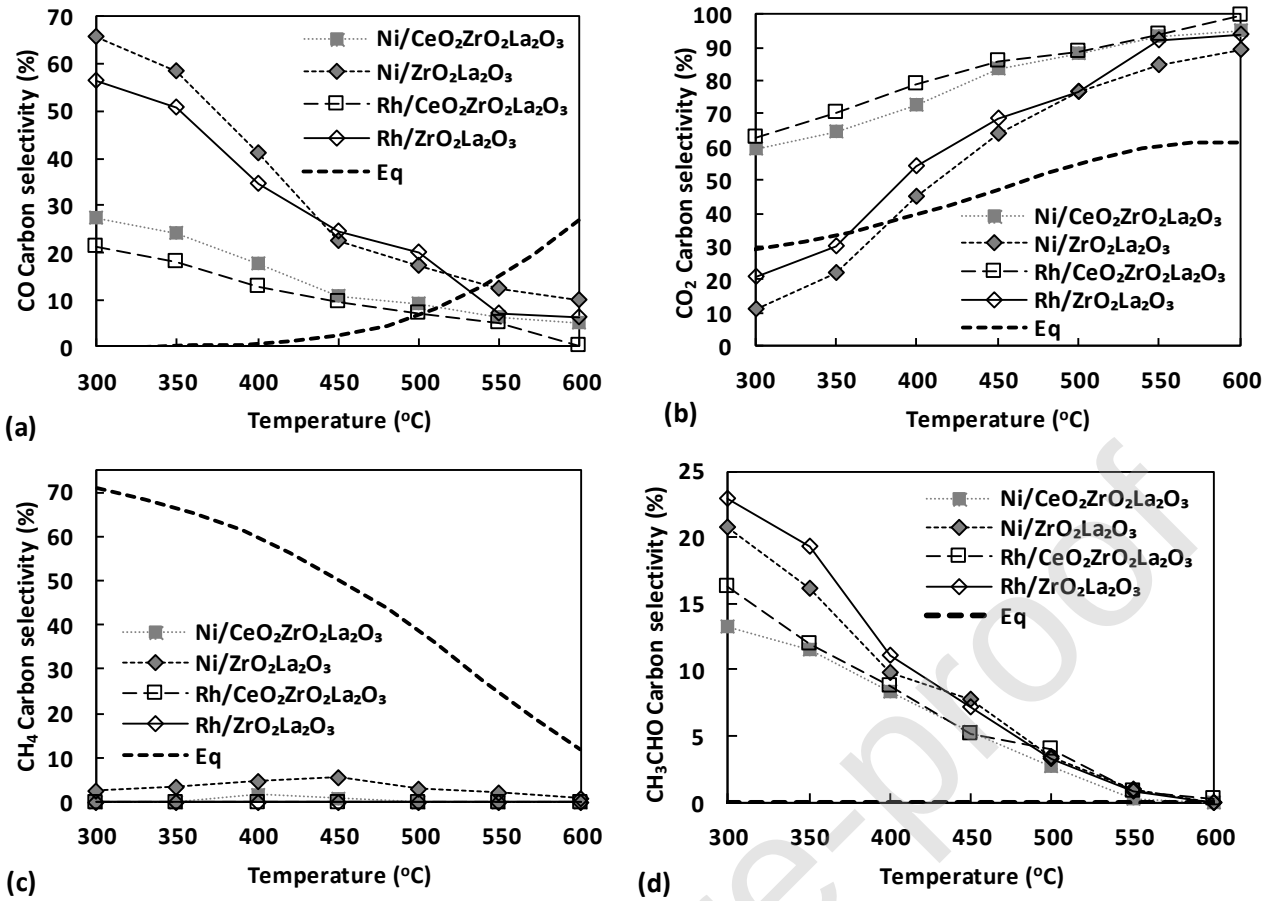

Figure 2. Temperature effect on carbon selectivities of CO (a), CO_2 (b), CH_4 (c) and CH_3CHO (d) for ESR over Ni and Rh based catalysts supported on (CeO_2)-ZrO_2-La_2O_3 compared with equilibrium ($W/F_{Eth,t0}$ = 91.88 g_{cat} s g_{Eth}^{-1}, P = 1.7 bara, S/C = 3).

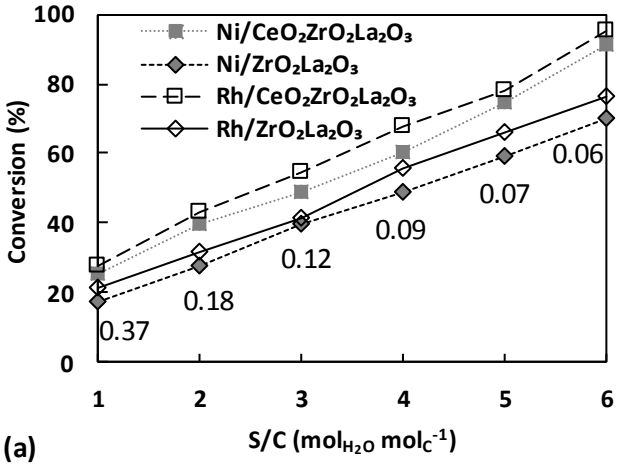

(a)

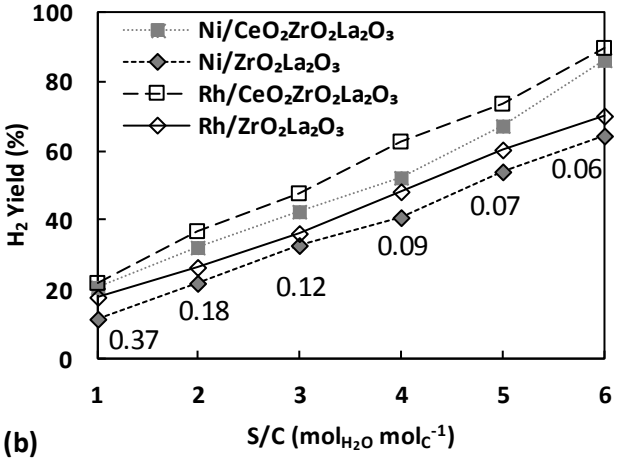

(b)

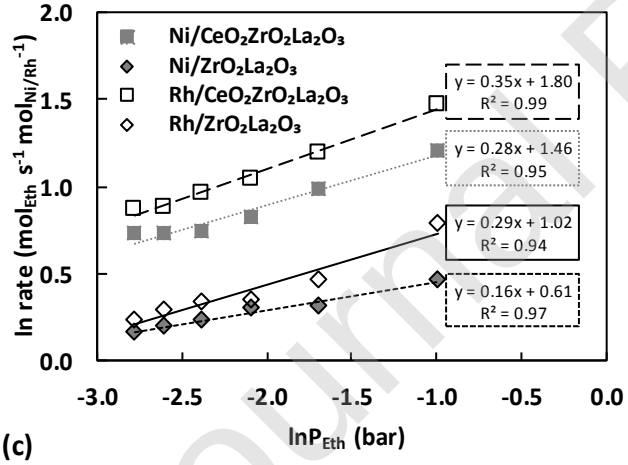

(c)

Figure 3. Partial pressure effect of ethanol on ethanol conversion (a) and H_2 yield (b) at 400°C over Ni and Rh based catalysts supported on (CeO_2)-ZrO_2-La_2O_3 presented as S/C variation with numbers on plots annotating the equivalent partial pressures of ethanol in bara, and ln reaction rate of ESR with respect to ln ethanol partial pressure (c) (P = 1.9 bara, GHSV = 1.78 s^{-1}).

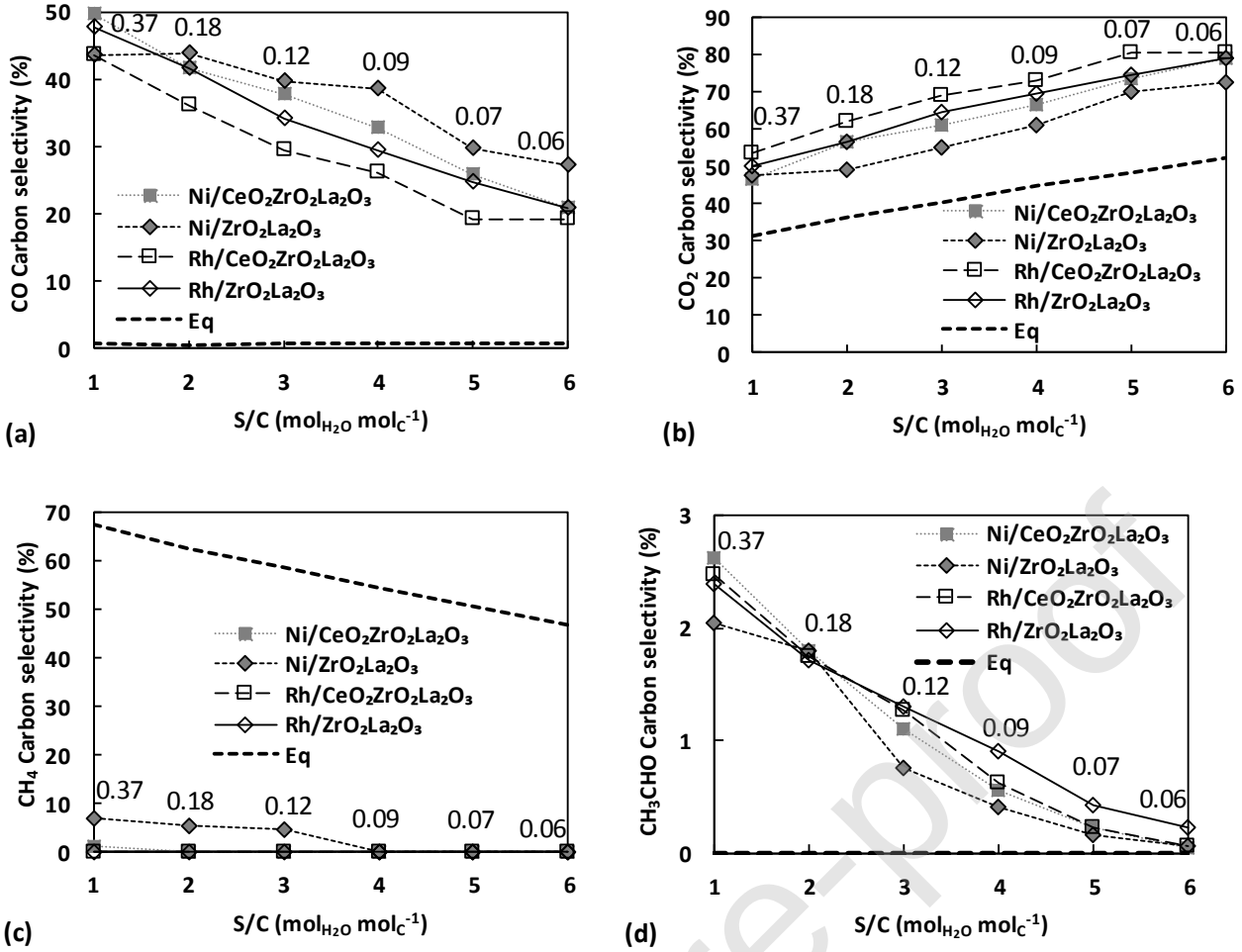

Figure 4. Partial pressure effect of ethanol on carbon selectivities of CO (a), CO_2 (b), CH_4 (c) and CH_3CHO (d) for ESR at 400°C over Ni and Rh based catalysts supported on (CeO_2)-ZrO_2-La_2O_3 compared with equilibrium, presented as S/C variation with numbers on plots annotating the equivalent partial pressures of ethanol in bara (P = 1.9 bara, GHSV = 1.78 s^{-1}).

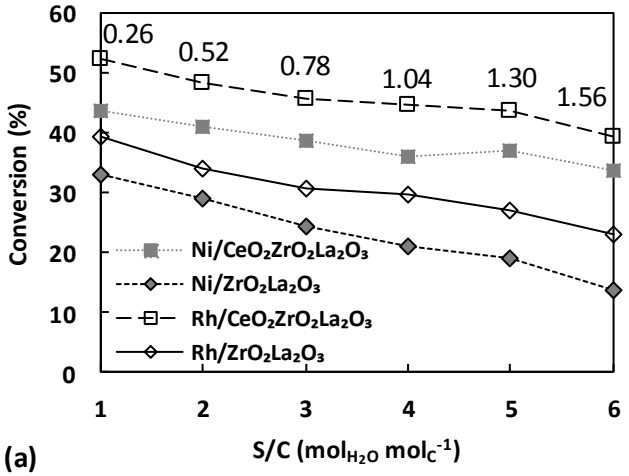

(a)

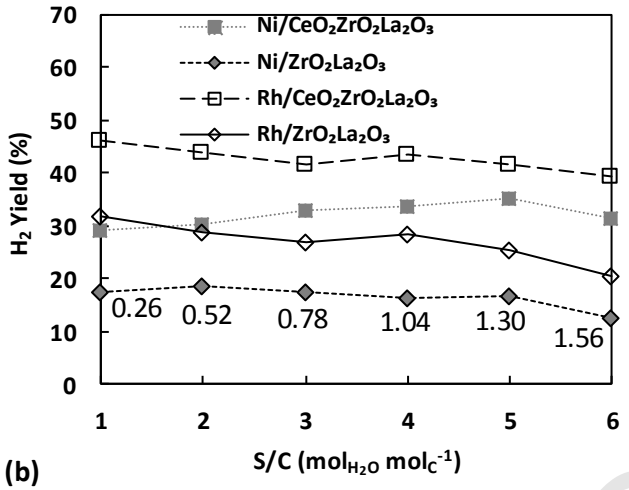

(b)

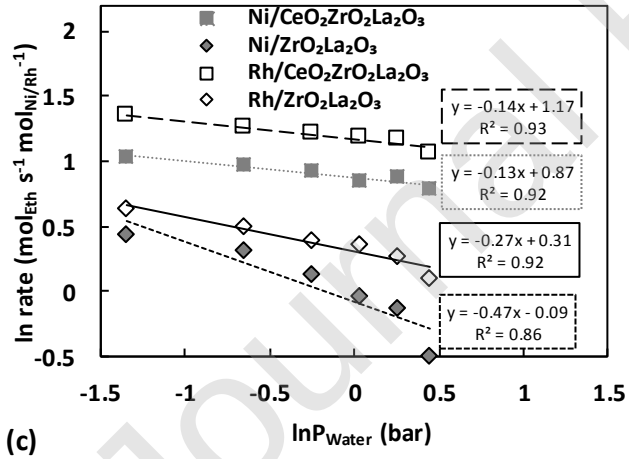

(c)

Figure 5. Partial pressure effect of water on ethanol conversion (a) and H_2 yield (b) at 400°C over Ni and Rh based catalysts supported on (CeO_2)-ZrO_2-La_2O_3 presented as S/C variation with numbers on plots annotating the equivalent partial pressures of water in bara, and ln reaction rate of ESR with respect to ln water partial pressure (c) (P = 1.9 bara, GHSV = 2.36 s^{-1}).

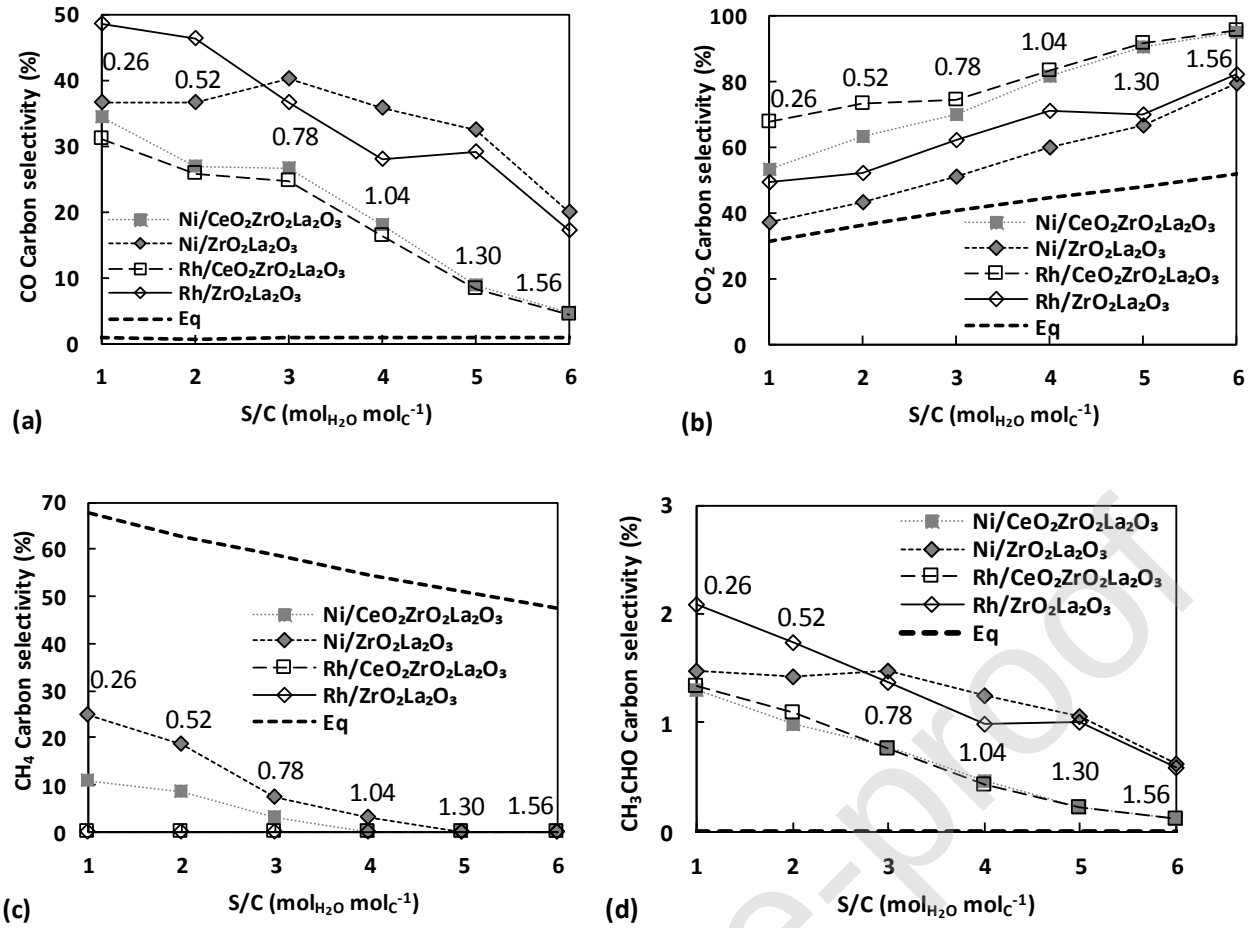

Figure 6. Partial pressure effect of water on carbon selectivities of CO (a), CO_2 (b), CH_4 (c) and CH_3CHO (d) for ESR at 400°C over Ni and Rh based catalysts supported on (CeO_2)-ZrO_2-La_2O_3 compared with equilibrium, presented as S/C variation with numbers on plots annotating the equivalent partial pressures of water in bara (P = 1.9 bara, GHSV = 2.36 s^{-1}).

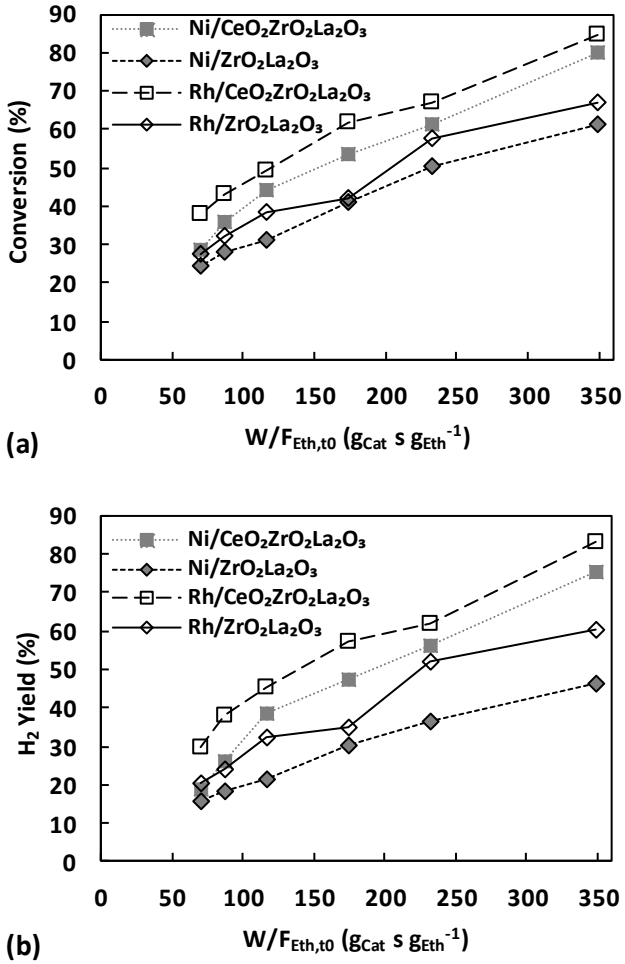

Figure 7. $W/F_{Eth,t0}$ effect on ethanol conversion (a) and H_2 yield (b) at 400°C over Ni and Rh based catalysts supported on (CeO_2)-ZrO_2-La_2O_3 (P = 1.8 bara, S/C = 3).

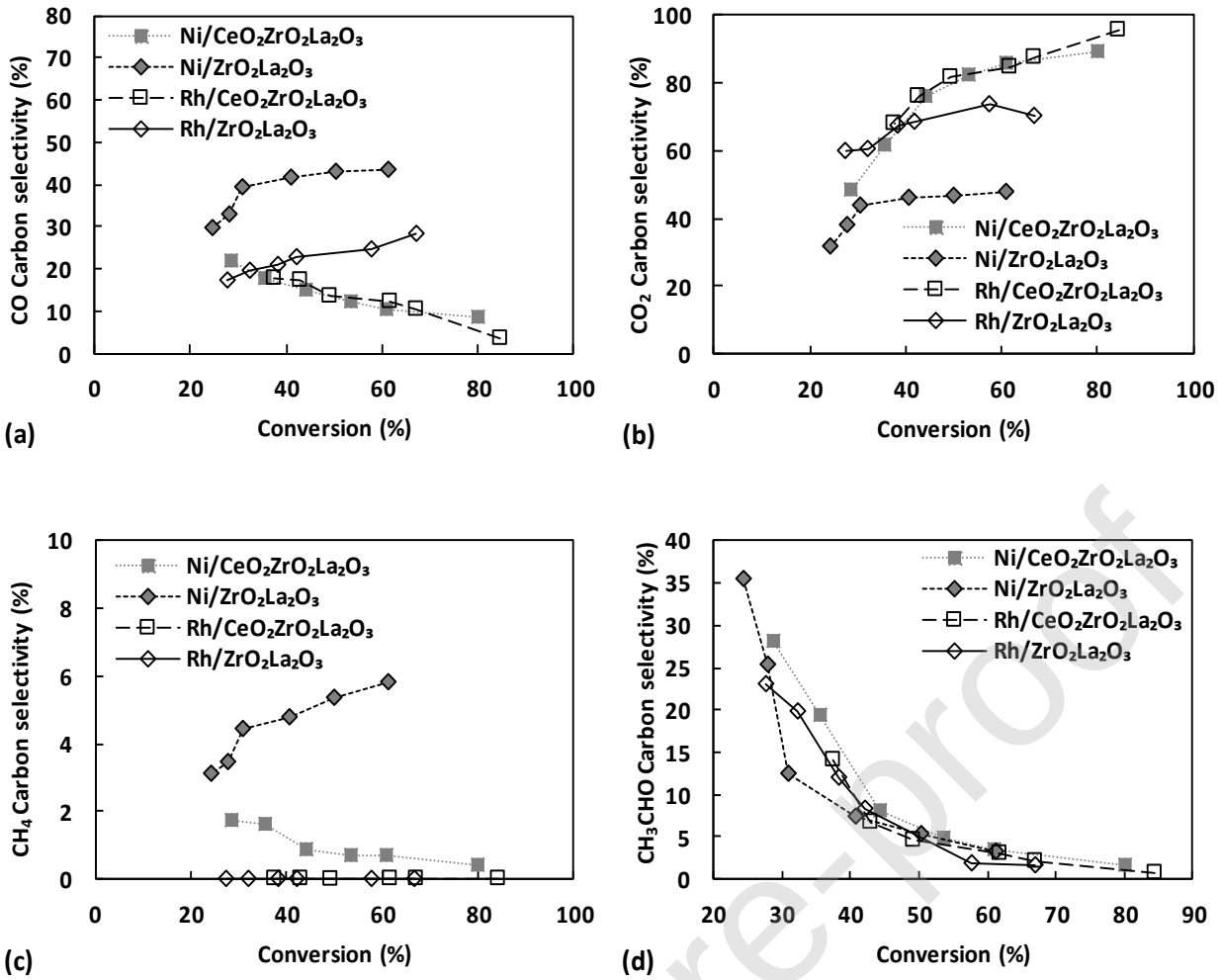

Figure 8. $W/F_{Eth,t_0}$ effect on carbon selectivities of CO (a), CO_2 (b), CH_4 (c) and CH_3CHO (d) at 400°C over Ni and Rh based catalysts supported on (CeO_2)-ZrO_2-La_2O_3, with the equivalent equilibrium values being CO: 1 %, CO_2: 38 %, CH_4: 61 % and CH_3CHO: 0 % (P = 1.8 bara, S/C = 3).

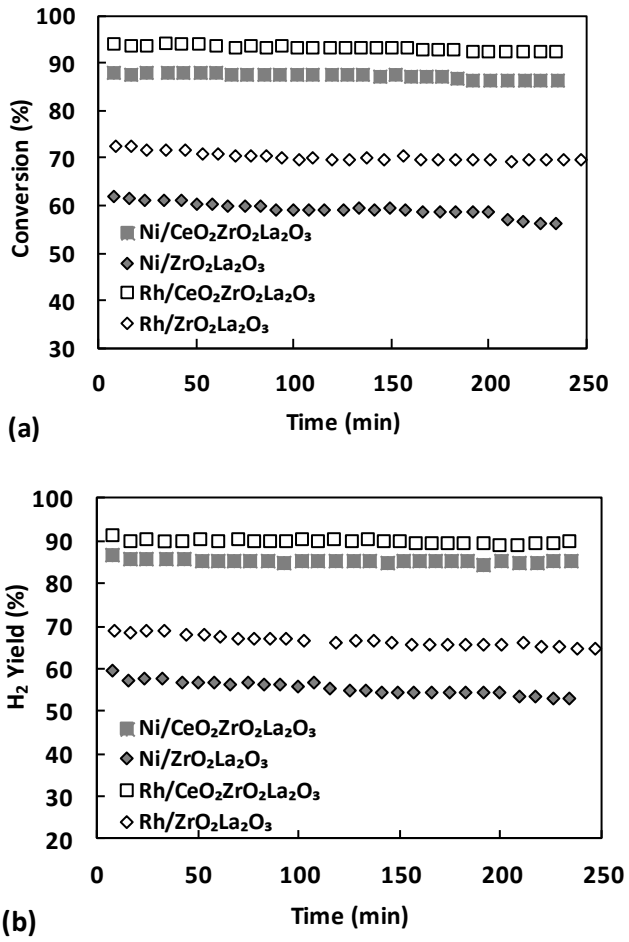

Figure 9. Ethanol conversion (a) and H_2 yield (b) against time-on-stream at 500°C over Ni and Rh based catalysts supported on (CeO_2)-ZrO_2-La_2O_3 ($W/F_{Eth,t0}$ = 358.57 g_{cat} s g_{Eth}^{-1}, S/C = 3).

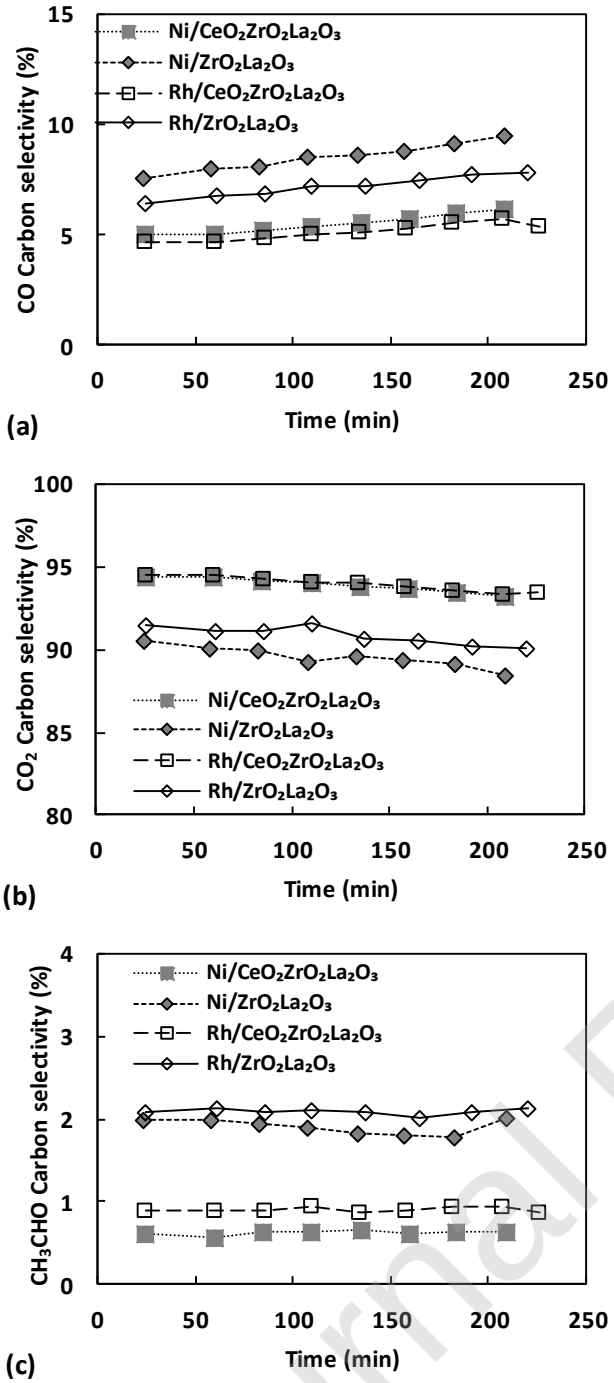

Figure 10. Carbon selectivities of CO (a), CO_2 (b) and CH_3CHO (c) against time-on-stream at 500°C over Ni and Rh based catalysts supported on (CeO_2)-ZrO_2-La_2O_3. Selectivity to CH_4 was zero for these experiments ($W/F_{Eth,t0}$ = 358.57 g_{cat} s g_{Eth}^{-1}, S/C = 3).

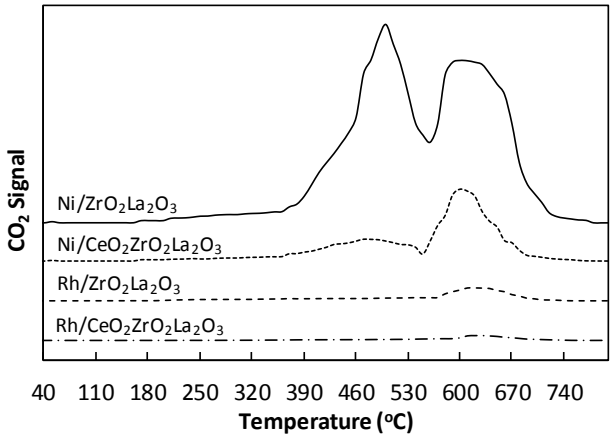

Figure 11. Temperature programmed oxidation profiles of spend catalysts following 4 h TOS experiments as described in Section 3.5.

Table 1. Mass based percentages of coke deposited on catalyst samples in terms of total carbon fed and of catalyst mass after 4 h TOS experiments as determined from the TPO analysis.

	Ni/CeO_2-ZrO_2-La_2O_3	Ni/ZrO_2-La_2O_3	Rh/CeO_2-ZrO_2-La_2O_3	Rh/ZrO_2-La_2O_3
Coke/Carbon fed	0.25%	0.63%	0.01%	0.09%
Coke/Catalyst mass	7.95%	24.57%	0.39%	3.51%